



Research on Longitudinal Damper Mitigation Measures for Super Kilometer-scale Cable-stayed Bridges

Laixu Li, Gao Zhang*, Yating Cao, Jie Liu

School of Environment and Civil Engineering, Chengdu University of Technology, Chengdu, Sichuan, China.

How to cite this paper: Laixu Li, Gao Zhang, Yating Cao, Jie Liu. (2024) Research on Longitudinal Damper Mitigation Measures for Super Kilometer-scale Cable-stayed Bridges. *Engineering Advances*, 4(2), 77-81.
DOI: 10.26855/ea.2024.04.001

Received: March 13, 2024
Accepted: April 10, 2024
Published: May 9, 2024

***Corresponding author:** Gao Zhang, School of Environment and Civil Engineering, Chengdu University of Technology, Chengdu, Sichuan, China.

Abstract

In this paper, a super kilometer-scale cable-stayed bridge was used as the research background. A nonlinear time-history analysis method was employed to study the seismic mitigation measures of installing longitudinal dampers between the main tower and the main girder. The influence of various damper parameters on the seismic response of the structure was analyzed, and a set of appropriate damper parameters was determined. The research findings demonstrated that the installation of longitudinal dampers can effectively reduce the seismic response of large-span cable-stayed bridges. The selection of damper parameters should consider the variation patterns of internal forces and displacements of the main structural components under seismic loading. Parameter optimization analysis was conducted based on the desired goals to achieve the intended seismic mitigation effect.

Keywords

Super kilometer-scale cable-stayed bridge, Seismic mitigation measures, Dampers, Nonlinear time-history analysis

1. Introduction

In recent years, the development of cable-stayed bridges in China has been rapid, with spans exceeding a kilometer due to their economic and versatile advantages. For large-span cable-stayed bridges, the method of the tower-pier constraint system has a significant impact on the seismic performance of the structure [1-4]. Cable-stayed bridge structures usually adopt floating systems, semi-floating systems [5], and fixed systems under seismic action, floating systems are prone to excessive seismic displacement response, while fixed systems exhibit significant seismic internal force response in the main tower [6-8].

In the longitudinal semi-floating system, different connection methods are often employed between the tower and girder to reduce structural seismic response [9-12]. Various connection methods have different mechanical characteristics. For instance, elastic cables only increase the stiffness of the structure in a certain direction without providing energy dissipation. Velocity-dependent viscous dampers generate damping force related to velocity, dissipating energy through the relative motion of the damper to increase additional damping without increasing structural stiffness, thus not constraining temperature deformations and creep of the bridge.

For super kilometer-scale cable-stayed bridges, the seismic response characteristics are different compared to large cable-stayed bridges with spans around 500 meters, which is due to the extraordinary span and flexibility of the super kilometer-scale cable-stayed bridge [13]. The seismic vulnerability also varies, necessitating different seismic strategies to reduce seismic response. For large-span cable-stayed bridges, reducing seismic response by extending the structural period is not suitable. When the structural period is long, further extending the natural period of vibration has no

significant effect on reducing seismic response and may increase structural displacement. Therefore, seismic mitigation for large-span bridges primarily focuses on increasing structural damping by incorporating energy dissipation devices to reduce internal forces and displacements.

2. Engineering Background

A certain super kilometer-scale double-tower three-cable-plane cable-stayed bridge is considered as the engineering background, with a main span of 1092 meters and a 462-meter side span on each side of the main span, an additional 140-meter auxiliary span is added on each side of the auxiliary navigation hole to meet navigation requirements while satisfying structural loading and beam end rotation requirements. The specific span arrangement of the main bridge is $(142+462+1092+462+142) = 2300$ meters, as shown in Figure 1. The main girder of the bridge adopts a combination of plate truss and steel truss, with a truss width of 35 meters, a truss height of 16 meters, a segment length of 14 meters, and a structural system of tower-girder separation and tower-pier fixed form. Bearings and dampers are installed between the towers and girders. The main girder features a new box-truss composite truss structure, with the lower chord of the truss composed of steel boxes of the same width as the main girder section, which also serves as the integral bridge deck. The upper chord of the highway bridge deck uses orthogonal anisotropic steel bridge panels and is integrated with the main truss.

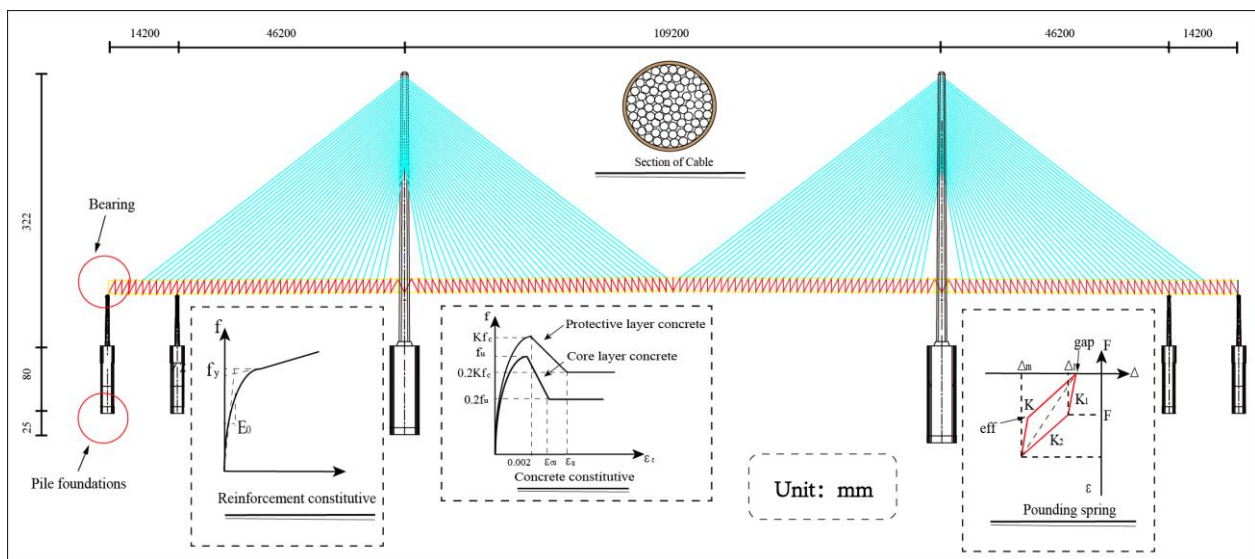


Figure 1. The overall layout diagram of the cable-stayed bridge (unit: mm).

3. Finite Element Model

The finite element model of the bridge is established using the OpenSees finite element program. The main girder, towers, and abutments are simulated using elastic beam-column elements, with rigid arm elements connecting the main girder nodes and cable suspension points. The cross-sectional properties of an elastic beam-column mainly include the moment of inertia, cross-sectional area, elastic modulus, and shear modulus. Use the MinMax material in OpenSees software to simulate the stress in a cable of a cable-stayed bridge, and use the Initial Strain Material to apply the initial strain to the cable. The combination of these two simulates the material properties of the cable. The inclined cable element is simulated using the Truss Element. Due to the focus of the study on the upper bridge structure, fixed constraints are applied at the bottom of the piers.

4. Damping Measures

It is proposed to use viscous dampers to reduce the longitudinal seismic response of the bridge. Two longitudinal viscous dampers are set between the lower crossbeam of the main tower and the main girder on each side of the main tower, totaling four viscous dampers along the longitudinal direction of the entire bridge. The mechanical relationship of the velocity-type viscous damper can be expressed as $F = CV^\xi$, where F is the damping force, C is the damping coefficient, V is the velocity, and ξ is the velocity exponent, which is generally chosen between 0.1 and 1.0 [14]. Under temperature and creep deformations, the reactive force of the damper is almost zero, which does not affect the normal functional use of the bridge structure. When the velocity exponent of the viscous damper is 1, the damping force is proportional to the velocity. At the maximum deformation velocity of the main tower, the damper provides the maximum damping

force, resulting in minimal tower deformation and internal forces. When the main tower deforms maximally, the damping force approaches zero. Therefore, the viscous damper does not significantly increase the forces on the main tower [15].

5. Nonlinear Seismic Response Analysis

The bridge is subjected to seismic response calculations using nonlinear time-history analysis. Three artificial seismic waves are synthesized based on the actual site conditions of the bridge, with the seismic input combination being "longitudinal + vertical," where the vertical seismic acceleration is 0.65 times the longitudinal seismic acceleration [16]. The structural internal forces and deformation responses under the action of the three seismic waves are calculated, and the maximum values are compared for analysis.

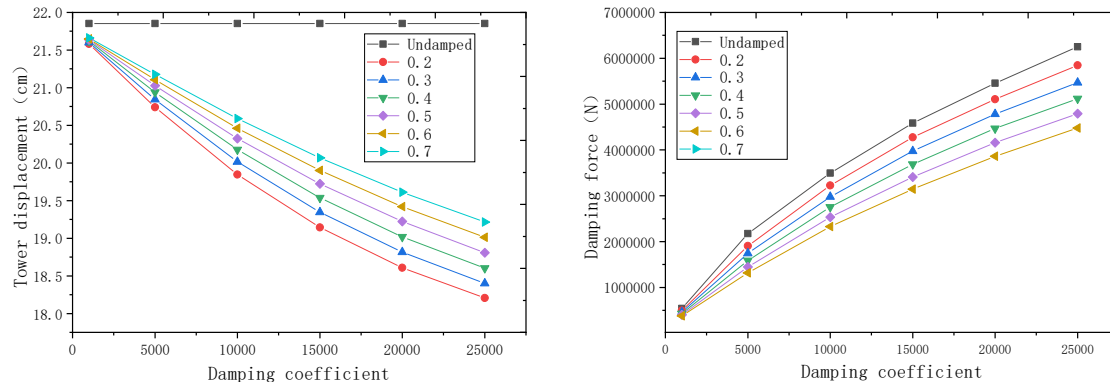


Figure 2. The force and displacement of the damper.

To study the damping and energy dissipation effects of the dampers on the structure, calculations, and analyses are conducted for both the longitudinal semi-floating system without dampers and multiple sets of different damper parameters. The velocity exponent ξ is varied from 0.2 to 0.7, and the damping coefficient C is set at 1000, 5000, 10000, 15000, 20000, and 25000, resulting in a total of 36 different damper parameter analyses. The seismic response analysis results for the major structural components are as follows. Figure 2 shows the variation of the maximum damping force and damping displacement at the dampers at the main tower when different velocity exponents and damping coefficients are set.

It can be observed from Figure 3 that when the damping coefficient is constant, the maximum damping force of the damper decreases with the increase in the velocity exponent. Conversely, when the velocity exponent is constant, the maximum damping force of the damper increases with the increase in the damping coefficient. The damping coefficient has a significant impact on the maximum damping force of the damper. When the damping coefficient is constant, the damper displacement increases with the increase in the velocity exponent. Conversely, when the velocity exponent is constant, the damper displacement decreases with the increase in the damping coefficient. Typically, a smaller velocity exponent of the damper results in better damping and energy dissipation effects, but it also leads to an increase in the damping force generated by the damper [17].

5.1 Sensitivity Analysis of Viscous Dampers Parameters

The key research points under the seismic action of the bridge mainly include two aspects: one is the internal forces of the critical structural parts, and the other is the displacement of the structure under seismic action [8]. The dampers set on the bridge are mainly used to suppress the longitudinal seismic action of the bridge, with the critical force location under longitudinal seismic action being the base of the tower. Meanwhile, the displacement analysis of the critical parts of the bridge under longitudinal action mainly focuses on the end of the beam and the top of the tower. Therefore, the impact of damper parameters on the seismic resistance of the bridge structure is analyzed by comparing the internal forces at the base of the tower with the displacements at the end of the beam and the top of the tower, combined with the magnitude of the maximum damping force of the damper, to ultimately determine the reasonable damper parameters for the bridge [18].

From Figure 3, it can be seen that when the velocity exponent of the damper is constant, with the increase in the damping coefficient C , the displacement at the end of the beam and the top of the tower monotonically decreases. When the damping coefficient is constant, the displacements at the end of the beam and the top of the tower decrease with the decrease in the velocity exponent. When the velocity exponent is constant, the displacements at the top of the tower and the end of the beam decrease with the increase in the damping coefficient. From the perspective of reducing the longitudinal displacements at the top of the tower and the end of the beam, it is advisable to choose a smaller value for the

velocity exponent and a larger value for the damping coefficient. It can be observed from the figure that the changes in the damping coefficient and velocity exponent of the damper have a relatively complex and varying impact on the bending moment and shear force of the main tower [19].

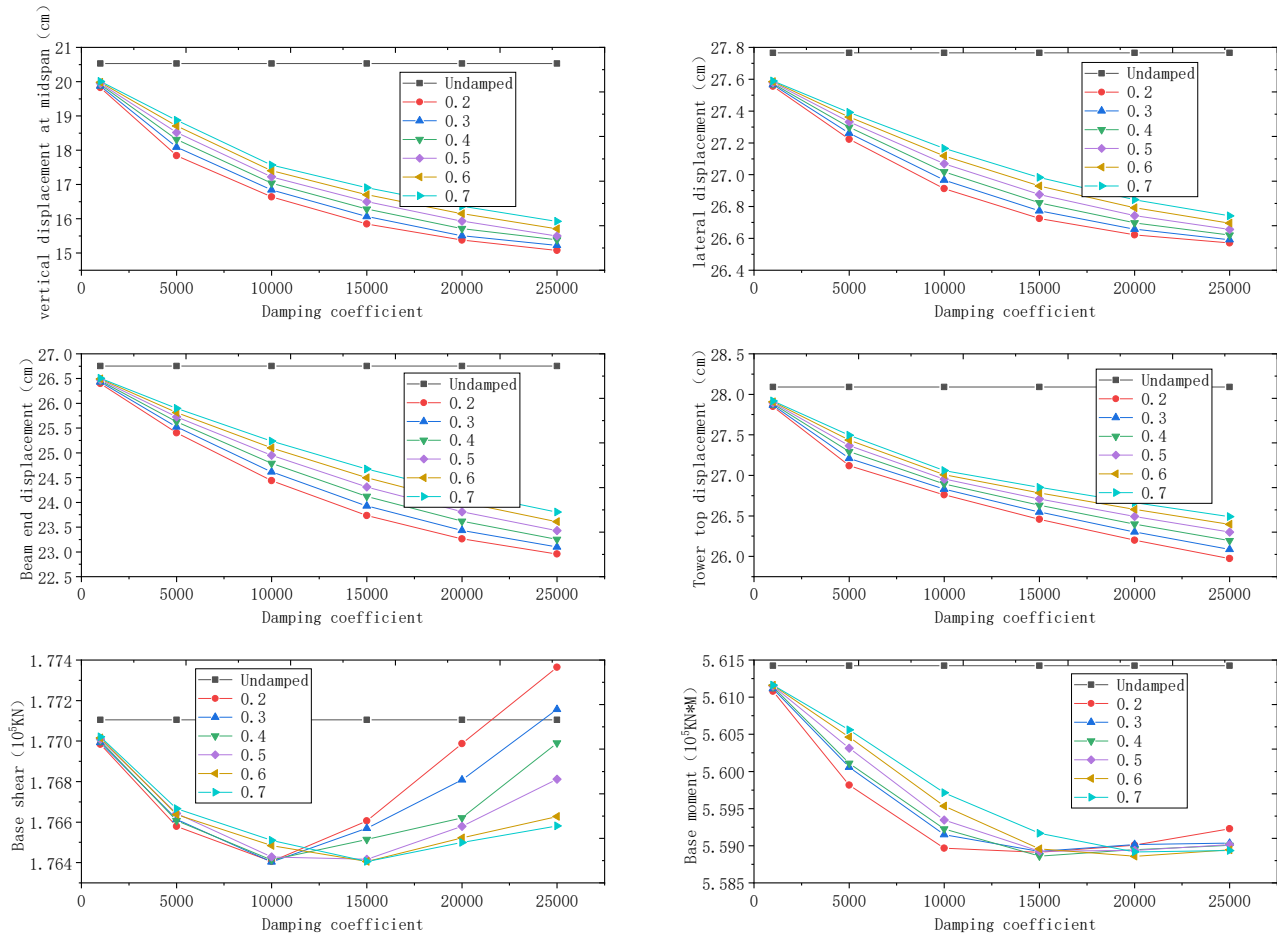


Figure 3. The impact of damper parameters on bridge structure.

When $0.2 < \zeta < 0.5$, the base shear at the tower decreases with an increase in the damping coefficient (C). However, when the damping coefficient exceeds 10000, the base shear starts to increase with further increases in the damping coefficient.

When $0.5 < \zeta < 0.7$, the base shear at the tower decreases with an increase in the damping coefficient. Similar to the previous case, when the damping coefficient exceeds 15000, the base shear starts to increase with further increases in the damping coefficient.

As the damping coefficient (C) increases, the base moment decreases. When the damping coefficient exceeds 15000, the base moment attenuates rapidly and eventually reaches a plateau with a slower rate of decrease.

From these patterns of change and the response quantities of critical structural parts, it can be seen that, under the premise of not increasing the internal forces of structural components, and minimizing the displacements at critical locations, the most suitable damper parameters are $C=15000$, $\zeta=0.3$.

6. Conclusion

Through the study of the longitudinal bridge shock absorption measures with set the dampers between the main tower and the main girder of the long-span cable-stayed bridge of over a kilometer, the following conclusions can be obtained:

(1) Compared with the longitudinal semi-floating system without dampers, the internal force and displacement response of the main components such as the main beam and main tower can be effectively reduced after installing the viscous dampers in the longitudinal direction of the bridge.

(2) Through the optimization analysis of the parameters of the viscous damper, the changes of the velocity index and damping coefficient of the damper have different degrees of influence on the internal force and displacement response of different components of the structure.

(3) For the parameters of the viscous dampers used in the bridge, the internal force and displacement response of the main components of the structure under the action of the earthquake should be comprehensively considered. For the bridge model in this paper, the damper with the damping coefficient $C=15000$, $\xi=0.3$ can be selected.

In short, to reduce the longitudinal seismic response of a large-span cable-stayed bridge, the measures of setting the damper between the tower and the beam can be taken. In order to obtain the best damping effect, the damper parameters should be optimized. Comprehensively consider the force and deformation of each key part of the structure and determine the appropriate damper parameters according to the optimization goal.

References

- [1] Dong Jun, Zeng Yongping, Zhang Jin, et al. Influence analysis of design parameters of seismic reduction and isolation of railway cable-stayed bridge with more than 250 m high-tower railway [J]. *Journal of Railway Science and Engineering*, 2022, 19(07):1963-1976. (In Chinese)
- [2] Guo Wenhua, Duan Binxin, Zhang Tingkui. Shock absorption analysis of viscous damper on coupling system of high-speed train and long-span cable-stayed bridge [J]. *China Railway Science*, 2022, 43(04):9-17. (In Chinese)
- [3] Lin K, Xu Y, Lu X, Guan Z, Li J. Cluster computing-aided model updating for a high-fidelity finite element model of a long-span cable-stayed bridge. *Earthq Eng Struct Dyn.*, 2020:1-20.
- [4] Han Q, Wen J, Du X, Huang C. Seismic response of single pylon cable-stayed bridge under scour effect. *J Bridge Eng.*, 2019, 24(6):05019007.
- [5] Subhayan D, Wojtkiewicz SF, Johnson EA. Efficient optimal design and design under-uncertainty of passive control devices with application to a cable-stayed bridge. *Struct Control Health Monit*, 2017, 24(2): e1846.
- [6] Xu Y, Wang R, Li Z. Experimental verification of a cable-stayed bridge model using passive energy dissipation devices. *J Bridge Eng.*, 2016, 21(12):04016092.
- [7] Guo W, Li JZ, Guan ZG. Shake table test on a long-span cable-stayed bridge with viscous dampers considering wave passage effects. *J Bridge Eng.*, 2021, 26(2): 04020118.
- [8] Yi J, Le JZ. Experimental and numerical study on seismic response of inclined tower legs of cable-stayed bridges during earthquakes. *Earthq Struct.*, 2019, 183: 180-94.
- [9] Wen JN, Han Q, Xie YZ, Du XL, Zhang J. Performance-based seismic design and optimization of damper devices for cable-stayed bridge. *Earthq Struct.*, 2021, 237: 112043.
- [10] Guan ZG, You H, Li JZ. An effective lateral earthquake-resisting system for long-span cable-stayed bridges against near-fault earthquakes. *Eng Struct.*, 2019, 196: 109345.
- [11] Zhou L, Wang X, Ye A. Shake table test on transverse steel damper seismic system for long span cable-stayed bridges. *Eng Struct.*, 2019, 179: 106-19.
- [12] Wang X, Fang J, Zhou L, et al. Transverse seismic failure mechanism and ductility of reinforced concrete pylon for long span cable-stayed bridges: Model test and numerical analysis. *Eng Struct.*, 2019, 189(15):206-21.
- [13] Li Lifeng, Liu Benyong, Zhang Chenxi, et al. Study on Seismic Mitigation Effect of Elastic Restraint Devices on Medium-Span Cable-Stayed Bridge Tower-Girder. *Earthquake Engineering and Engineering Vibration*, 2013, 33(1): 146-152. (In Chinese)
- [14] Li Zhongxian, Zhou Li, Yue Fuqing. Seismic Collision Analysis and Parameter Design of Urban Bridge Viscous Dampers [J]. *Earthquake Engineering and Engineering Vibration*, 2006, 26(5): 195-200. (In Chinese)
- [15] Mahendra P Singh, F. ASCE, Navin P Verma, et al. Moreschi, Seismic analysis and design with Maxwell dampers [J]. *Journal of Engineering Mechanics*, 2003, 129(3): 273-282. (In Chinese)
- [16] Yang Xiwen, Zhang Wenhua, LI Jianzhong. Seismic design for long-span cable-stayed bridges in transverse direction [J]. *Earthquake Engineering and Engineering Dynamics*, 2012, 32(1): 86-92. (In Chinese)
- [17] Wang Zhiqiang, Hu Shide, Fan Lichu. Study on Parameters of Viscous Dampers for Donghai Bridge [J]. *China Journal of Highway and Transport*, 2005, 7(3): 37-42. (In Chinese)
- [18] Wu Shengping, Zhang Chao, Fang Zhenzheng. Design schemes and parameter regression analysis of viscous dampers for cable-stayed bridge [J]. *Bridge Construction*, 2014, 44(5): 21-26. (In Chinese)
- [19] Bougteb Y, R AY T. Choice between series and parallel connections of hysteretic system and viscous damper for seismic protection of structures [J]. *Earthquake Engineering and Structural Dynamics*, 2018, 47(1): 237-244.